Minimizing the Effect of IMU Misplacement With a Functional Orientation Method

Julien A. Mihy[1], Mayumi Wagatsuma[1], Stephen M. Cain[2], Jocelyn F. Hafer[1]
[1]University of Delaware, [2]West Virginia University

Key words: wearable sensors, gait, real-world, alignment

Abstract

Background Functional orientation orients inertial measurement unit (IMU) data (i.e., linear accelerations and angular velocities) to interpretable reference frames. To confidently collect reliable out-of-lab data, it is important to determine the extent to which we can correct for sensor placement variability. **Research Question** To what extent does a functional orientation method minimize the effect of variability in sensor placement on IMU data? **Methods** Twenty healthy adults (10 younger 28.2±3.7 years, 10 older 60.8±3.3years) walked overground at preferred speed in a lab. Three IMUs were placed per segment on the pelvis, thigh, shank, and foot. IMU data were oriented using an assumed orientation and two versions of a walking-based functional orientation (X-functional anchored to axis of rotation and Z-functional anchored to gravity). Segment angular excursions were calculated for each orientation method and compared between groups and sensor placements. **Results and Significance** No significant interaction was found between sensor placement and group for any orientation method. For assumed orientation, segment angular excursion differed between sensor placements for at least 15% and up to 95% of the gait cycle, depending on segment. For both functional orientation methods, foot and shank excursions did not differ between sensors. Thigh excursion differed only for the X-functional orientation from 27-68% of the gait cycle. Neither functional orientation fully corrected for differences at the pelvis leaving significantly different excursions between 24-50% of the gait cycle. Functional orientation can reliably correct for variability in lower extremity IMU sensor placement. These methods can enable repeatable real-world IMU data collection in settings where sensors may move within or between days. Performing functional orientation periodically throughout a day can minimize the effect of sliding or rotating of the sensors on IMU-calculated gait measures and give in-lab quality gait data throughout hours of real-world activity to better understand the true movement of participants.

1. Introduction

The use of inertial measurement units (IMUs) for gait research has increased in the last decade, largely because IMUs allow for affordable and portable measurement of movement. Despite the portability of IMUs, most studies using IMUs collect data in labs or controlled, observed settings. Several challenges limit the use of IMUs in unobserved, free-living settings. One major hurdle to free-living data collection is the ability to reliably orient IMU data to an interpretable reference frame in the absence of direct observation of sensor placement or calibration procedures.

Several methods exist for orienting IMU data to interpretable (e.g., anatomical or functional) reference frames [1,2]. Reference frames can be created using various methods, the most common of which are assumed, functional, and model-based orientation methods. Assumed orientation, which relies on an IMU's hardware axes being physically aligned with anatomy when place on a body segment, requires no postprocessing to reorient IMU data. However, the accuracy of axis orientation in this method is sensitive to sensor placement and reliant on the assumption that sensors on the body surface align with underlying anatomy [3–5]. Functional orientation uses participant motion to orient IMU data to specific axes (e.g., approximately frontal, sagittal, or transverse) [6–8]. Functional orientation methods only

require simple motions to implement, but the orientations of the axes depend on the participant's performance of the orientation procedure. Model-based methods use kinematic or statistical models of lower extremity degrees of freedom to orient data to anatomical reference frames. While model-based orientation minimizes reliance on precise sensor placement, these methods are computationally intensive, rely on physical and statistical assumptions of human movement, and may require extensive training data [9–12]. Because of assumptions about sensor orientation for assumed orientation and requirements of advanced computations or additional data sources for model-based orientation, functional orientation methods appear best-suited to free-living data collection.

Functional orientation can be applied in several ways. Participants may perform a series of controlled segment rotations to orient IMU data to sagittal, frontal, and transverse anatomical axes [7,11,13]. Accurate axis orientation thus relies on a participant's ability to precisely perform controlled motions about each axis. Alternatively, a combination of static and dynamic data may be used to define functionally relevant axes (e.g., vertical and medial-lateral) [14–18]. This procedure doesn't give anatomical sagittal, frontal, or transverse axes. However, a walking-based functional orientation can give accurate sagittal plane joint angles and eliminates the need for precise motions about each axis for orientation [16]. Walking and standing occur frequently during daily life and thus lower extremity IMU data could be oriented to consistent vertical and medial-lateral axes whenever a participant walks, regardless of actual sensor location or orientation on a segment.

The purpose of this study was to determine to what extent a walking- and toe-touch-based functional orientation method minimizes the effect of differences in IMU sensor placement on segment angular excursions during walking. Because body composition and gait characteristics change with age and might affect sensor motion characteristics, a secondary purpose was to determine whether age influences the effect of functional orientation.

2. Methods

2.1. Participants

Twenty healthy adults, 10 young (5 male, 28.2±3.7 years) and 10 older (5 male, 60.8±3.3years) participated in this study. All subjects had a BMI <30 kg/m^2, were able to walk for 30 min without assistive devices, and had no history of major traumatic injury, surgery, or chronic pain in the back or lower extremities. All individuals completed IRB-approved consent before participating in any study procedures.

2.2. Data Collection

Three IMUs [Opal v2, APDM] were placed on the pelvis and right thigh, shank, and foot. The three sensors were placed to represent a standard, recommended sensor placement (typical), a sensor placement that was shifted along a segment relative to typical, and a sensor placement that was rotated about a segment relative to typical (Figure 1). The shifted and rotated locations represent differences in placement that might occur when non-experts (i.e., participants) place sensors or if sensors shift position throughout a long data collection. Pelvis sensors were placed over the sacrum (typical), lateral to sacrum (shifted), and medial to the right anterior superior iliac crest (rotated). Thigh and shank sensors were placed at the midpoint on the lateral aspect of the segment (typical), proximal to typical (shifted), and on the anterior aspect of the segment (rotated). Foot sensors were placed on participants' shoes on the dorsum of the foot (typical), on the lateral instep (shifted), and on the heel (rotated).

IMU data were collected continuously as participants completed functional tasks (walking and toe-touches) and walked overground at a self-selected preferred speed. Walking trials were collected as part of a larger study where participants completed 10 successful trials (full foot strike on a force plate) at +/- 5% of preferred speed.

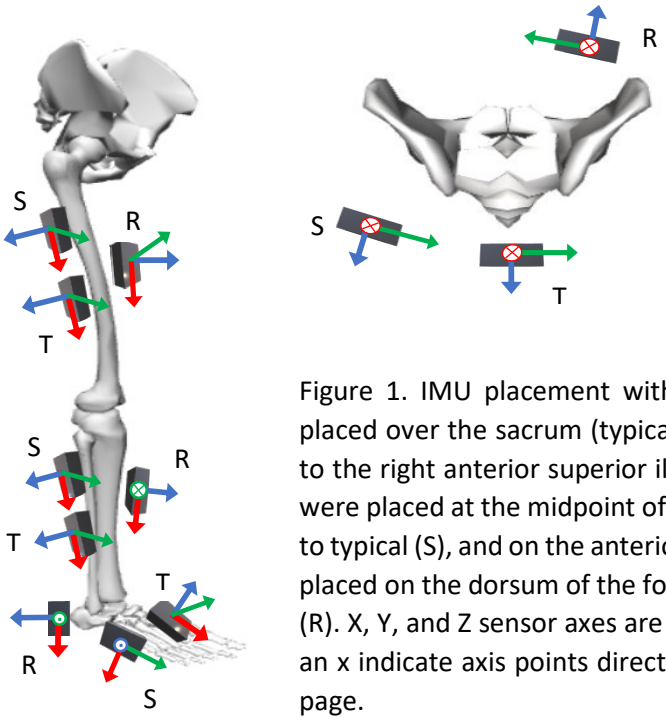

Figure 1. IMU placement with hardware sensor axes. Pelvis sensors were placed over the sacrum (typical, T), lateral to sacrum (shifted, S), and medial to the right anterior superior iliac crest (rotated, R). Thigh and shank sensors were placed at the midpoint of the lateral aspect of the segment (T), proximal to typical (S), and on the anterior aspect of the segment (R). Foot sensors were placed on the dorsum of the foot (T), on the lateral instep (S), and on the heel (R). X, Y, and Z sensor axes are red, green, and blue, respectively. Circles with an x indicate axis points directly into of the page while dots point out of the page.

2.3. Data processing

2.3.1. Reference frame orientation

Processing began by identifying the data that included functional movements and postures: quiet standing, a short bout of straight-line walking, and toe touches. Functional tasks were identified using the typical pelvis and shank sensors' linear acceleration and angular velocity data in the sensor hardware reference frames (Figure 2). A short range of pelvis raw linear acceleration and angular velocity data centered around zero identified quiet standing. Toe touches included roughly five cycles of pelvis sensor angular velocities about the mediolateral axis. Walking was identified as three to five cycles of shank angular velocity data about the mediolateral axis. Toe touch and walking data were selected using repeating signal peaks to obtain full cycles. After functional data identification, we oriented IMU data for each sensor to an assumed reference frame and to two versions of a functional reference frame.

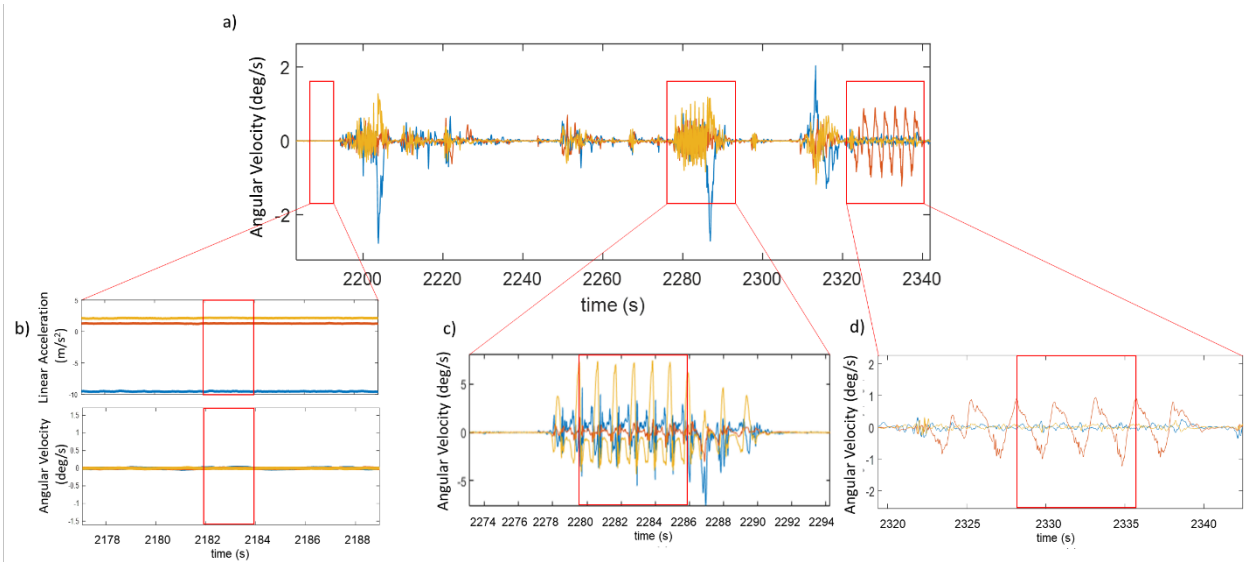

Figure 2. Calibration section of full data collection (a) including quiet static standing (b), walking (c), and toe touches (d). a) Pelvis raw angular velocity to determine ranges of data for static standing, walking, and toe touches. b) Pelvis raw acceleration (top) and angular velocity (bottom) used to determine frame with least movement for defining quiet standing. c) Shank raw angular velocity, selecting peak to peak for full gait cycles. d) Pelvis raw angular velocity, selecting peak to peak for full toe touch cycles.

Assumed orientation:

Typical IMU placements represented where a researcher would place sensors and how sensors would be assumed to be placed in unobserved data. This orientation assumes that specific sensor hardware axes align with anatomical axes (e.g., for the thigh, the sensor +Z axis points laterally, thus, the +Z axis was assumed to align with the medial-lateral anatomical axis for all placements). For each segment, the typical sensor axis that aligned most closely with the medial-lateral anatomical axis was assumed to be the medial-lateral axis for all sensors on that segment (+Z for thigh and shank, +Y for pelvis, -Y for foot) (Figure 3a).

World orientation:

World orientation aligned the vertical (Z) axis with gravity and makes X and Y axes orthogonal in the horizontal plane (Figure 3b). Orientation of IMU data to the world reference frame was performed with a manufacturer-provided Kalman filter (APDM, Inc.).

Functional orientation:

Functional orientation created reference frames where one axis aligns with the primary axis of segment rotation during walking or toe-touches (medial-lateral) and another axis aligns with the primary axis of linear acceleration during static standing (longitudinal). Initial axis orientations were defined by setting the longitudinal (Z) axis orientation as parallel to gravity during static standing (i.e., longitudinal axis aligned with average linear acceleration vector) and setting the medial-lateral (X) axis orientation as the primary axis of rotation during straight-line walking (thigh, shank, foot) or toe-touches (pelvis) using

principal component analysis. An anterior-posterior (Y) axis was created by crossing the longitudinal and medial-lateral axes (Figure 3c).

Because the initial longitudinal and medial-lateral axes are not perpendicular, one of these two axes must be re-oriented to create an orthogonal reference frame. Thus, there are two ways to define the final reference frame. We created an X-functional reference frame by re-orienting the longitudinal axis as X×Y and a Z-functional reference frame by re-orienting the medial-lateral axis as Y×Z.

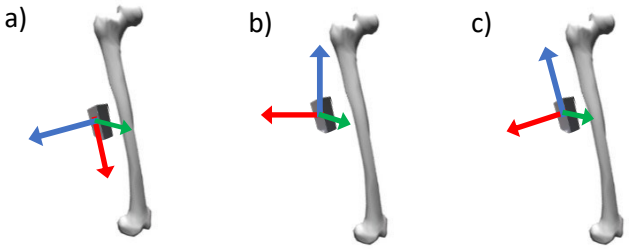

Figure 3. a) IMU hardware axes b) World oriented axes, Z aligned with gravity and X and Y orthogonal in the horizontal plane c) Functionally oriented axes, X and Z aligned by walking and quiet standing respectively.

2.3.2. Walking identification

We extracted bouts of walking from continuous IMU data based on repeated oscillations of the shank sensor (Figure 4). First, data from each axis of the shank sensor raw angular velocity signal was passed through a fast Fourier transform (FFT). Then, the frequency power from all three axes were summed to determine the total power density. A five second moving window was used to identify ranges of high-power density within frequencies representative of shank oscillations during walking (0.5 and 2.2 Hz). Consecutive identified sections of walking less than 2.5 seconds apart were combined.

Individual strides were identified using data from the foot sensor. Foot world oriented vertical acceleration data were passed through a one-dimensional continuous wavelet transform. Absolute value of the first (i.e., highest-frequency) wavelet was low-pass filtered with a second order Butterworth filter at 4Hz. Signal peaks above a threshold (half the median magnitude of the peaks of the filtered signal) were defined as gait events. Heel strike and toe off were defined using the slope of the vertical foot sensor displacement at the time of each identified gait event. A negative slope indicated heel strike and positive slope indicated toe off. A stride was created if gait events included a consecutive heel strike - toe off - heel strike pattern.

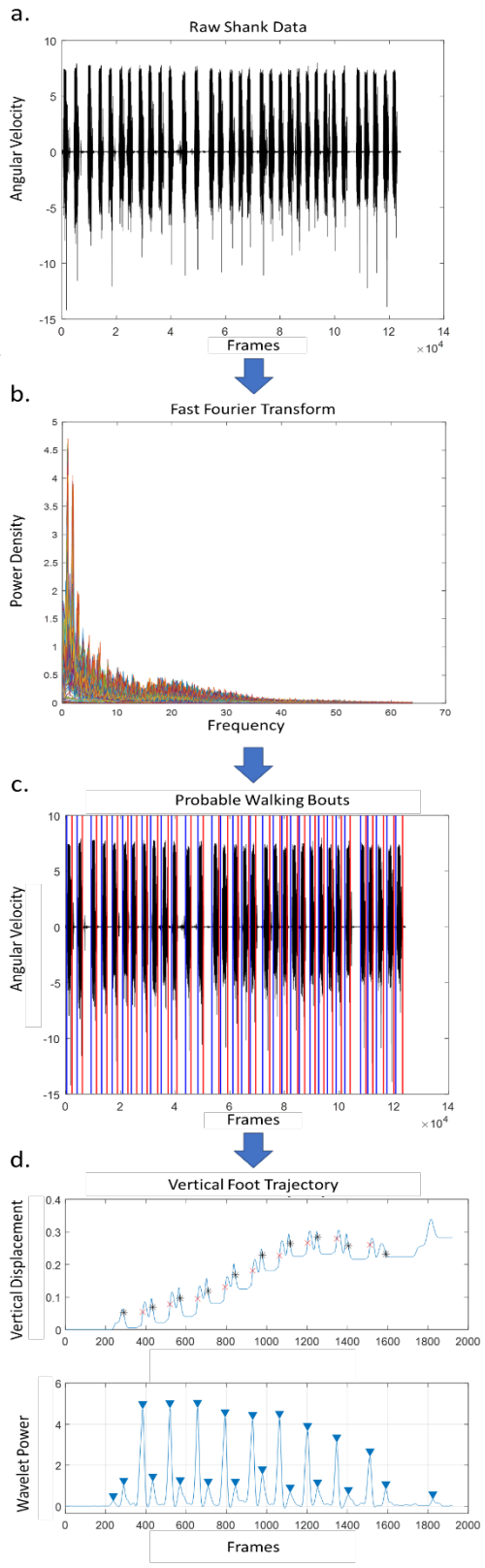

Figure 4. a) range of raw shank angular velocity data that may contain walking. b) Fast Fourier transform of 5 second windows of data. c) Identified ranges of walking based on windows with a frequency power greater than 1/3 the maximum power and a frequency between 0.5 and 2.2 Hz. d) Top plot visualizes the foot vertical displacement. Black * represents heel strikes and red x represents toe offs. Timing of gait events is based on spikes in the power of the highest frequency signal from a continuous wavelet transform. Type of gait event is based on slope of vertical displacement at time of frequency power spike (negative = heel strike).

This analysis used all straight-line steady-state strides including those without successful force plate strikes and outside of preferred speed. On average, 33 strides were included per participant (range = 25-60). Steady-state, straight-line strides were those with a consecutive inter-stride velocity difference of less than 0.1 m/s and angular deviation of less than 10 degrees. Stride displacement was calculated as the double integral of the typical foot sensor linear acceleration in the world reference frame. Stride length was the net displacement in the horizontal direction between heel strikes. Stride velocity was calculated by dividing stride length by the time between heel strikes. Stride angular deviation was calculated by taking the inverse tangent of the displacement in the two horizontal world reference axis directions.

2.4. Outcome variable calculation

Segment angular excursions about the medial-lateral axis were calculated for every stride for each sensor (typical, shifted, rotated) for each of the three reference frames: assumed, X-functional, and Z-functional. Segment angular excursions were calculated by integrating the angular velocity between consecutive heel strikes. For the functional orientation methods, we integrated angular velocity about the medial-lateral (X) axis. For the assumed orientation method, we integrated angular velocity about the sensor axis that was assumed to align with the anatomical medial-lateral axis based on typical placement (+Z for thigh and shank, +Y for pelvis, -Y for foot). An average segment angular excursion time series per orientation technique per IMU location per subject was included in statistical comparisons.

2.5. Statistics

For each orientation method (assumed, X-functional, Z-functional), segment excursion time series data were compared across each of the three IMU locations (typical, shifted, and rotated) and between groups (young and older) using a continuous 2-way ANOVA via statistical parametric mapping (SPM; α=.05). Where significant interactions were found, one-way ANOVAs via SPM were used to determine if excursions differed across placements within a group. T-tests via SPM were used to examine post-hocs where significant main effects were found.

3. Results

No significant interaction was found between age and sensor location for any segment ($p>.05$). A significant main effect was found for sensor location for the assumed orientation for all segment excursions as well as the pelvis and thigh X-functional orientation and pelvis Z-functional orientation (all $p<.001$; Figure 5).

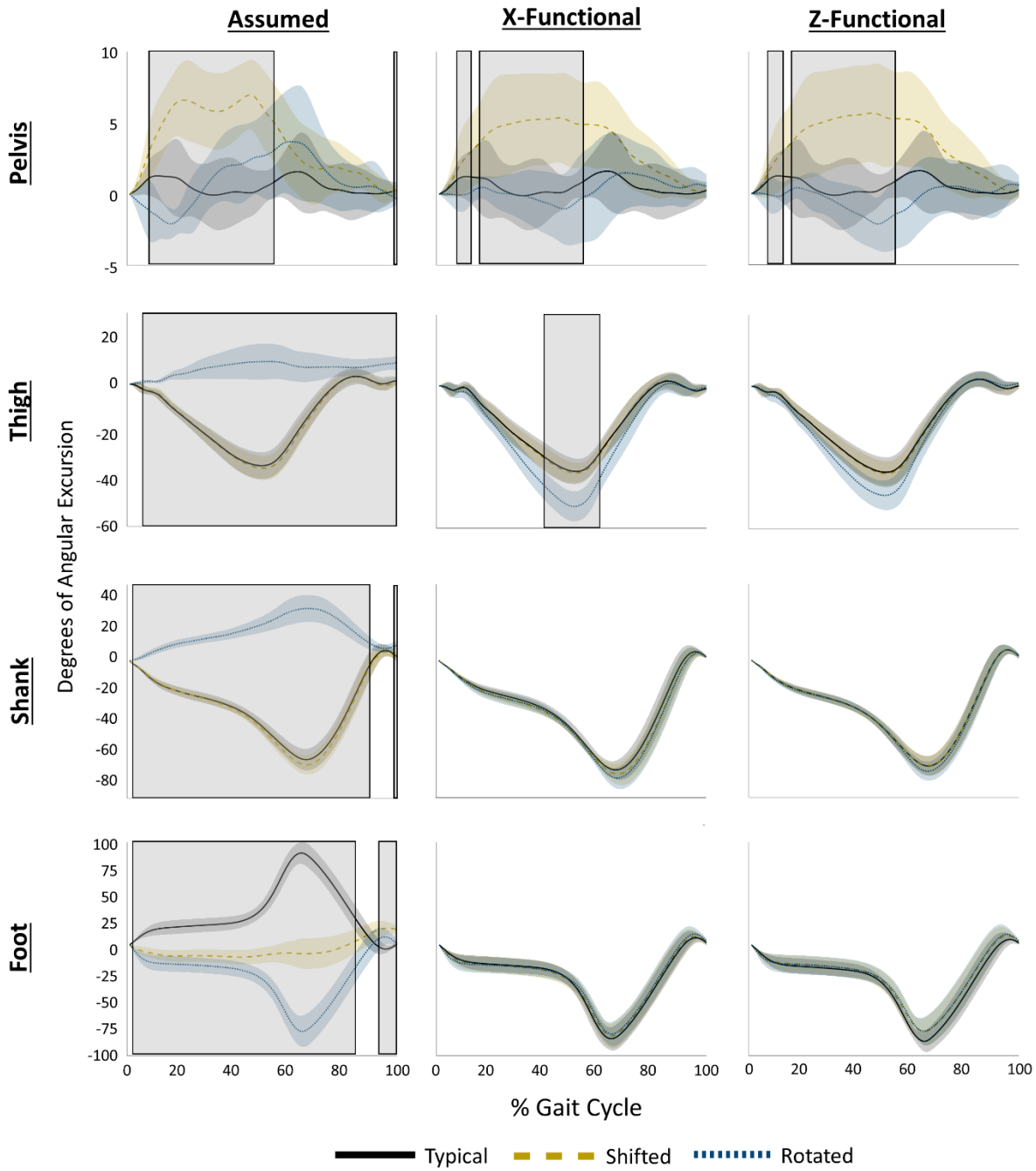

Figure 5. Segment excursions (mean and SD) from each sensor and orientation method. Boxes indicate significant differences between sensor locations. Solid black line = typical sensor location, yellow dashed line = shifted, and blue dotted = rotated (see figure 1).

Assumed orientation:
For the assumed orientation, pelvis angular excursions differed between typical and shifted locations (7-50% and 99-100% gait cycle), between typical and rotated (33-47% & 99-100 % gait cycle), and between rotated and shifted locations (8-24% & 99-100% gait cycle). Thigh angular excursion differed between typical and rotated locations and shifted and rotated locations (5-100% gait cycle for both comparisons). Shank angular excursion differed between typical and rotated locations (1-85% and 93-100% gait cycle) and shifted and rotated locations (1-87% and 97-100% gait cycle). Foot angular excursion differed between typical and shifted (1-83% and 93-100% gait cycle), typical and rotated (1-86% and 95-97% gait cycle), and shifted and rotated locations (43-83% and 97-100% gait cycle).

Functional orientations:
X-functional oriented angular excursions differed between the pelvis typical and shifted locations (24-49% gait cycle), between typical and rotated locations (4-11% & 17-59% gait cycle), and between rotated and shifted locations (4-12% & 17-59% gait cycle). Thigh angular excursion differed between typical and rotated (28-65% gait cycle) and shifted and rotated locations (27-68% gait cycle). No differences in X-functional angular excursion were found between sensor locations for the shank or foot.

Z-functional oriented angular excursions differed between the pelvis typical and shifted locations (24-50% gait cycle), between typical and rotated locations (4-11% & 44-51% gait cycle), and between shifted and rotated (6-12% & 17-60% gait cycle). No differences in Z-functional angular excursion were found between the thigh, shank, or foot sensor locations.

4. Discussion

The primary aim of this project was to determine the extent to which a walking- and toe-touch-based functional orientation method minimizes the effect of differences in IMU sensor placement on segment angular excursions during walking. The secondary aim of this project was to determine whether the effect of functional orientation differed by age. The functional orientation method reduced differences in angular excursion between IMU placements. While differences in angular excursion for assumed orientation method encompassed up to 45% of the gait cycle for the pelvis, 95% for the thigh, 92% for the shank, and 93% of the foot, functional orientation reduced these ranges to be 42% of the gait cycle for the pelvis, 29% for the thigh, and 0% for the shank and foot. These trends did not change with age.

X- and Z-functional orientation methods similarly minimized inter-placement excursion differences compared to the assumed orientation. The effect of the functional orientation method is best demonstrated by the similarity of the data between all sensor locations for the foot and shank sensors (Figure 4). These segments had the largest ranges of significantly different assumed orientation angular excursions across sensor locations, but had no differences in angular excursion between sensors once functionally oriented. This may be due to the foot and shank best mimicking a rigid body making the magnitude of the angular velocity similar regardless of sensor location on the segment.

The orientation methods performed similarly to each other for the thigh except that Z-functional performed better than X-functional orientation at correcting for the rotated sensor location. This difference may be due to the larger amount of soft tissue artifact and muscle contraction motion found on the anterior vs lateral thigh. Soft tissue artifact, particularly from contraction of the quadriceps, likely adds angular velocity signal about a non-medial-lateral axis, thus influencing the overall primary axis of rotation of the segment-mounted IMU. The Z-functional orientation likely performed better for the rotated position due to weighting the longitudinal axis more heavily than the soft-tissue-influenced

medial-lateral axis. Differences in pelvis angular excursion were lessened with functional orientation, but differences still existed between the shifted sensor location and both the typical and rotated locations for both functional orientation methods from mid to late stance. The shifted sensor's motion during toe-touches could have been influenced by deformation of the gluteal muscles during toe-touches. Therefore, sensors should be placed away from areas that are subject to deformation from large muscles or soft tissue.

In this study, IMU placement represented sensor misplacements or movement during unobserved activity. In practice, small shifts or misplacements of sensors can be hard to identify when processing unobserved data. The rotated position is an extreme example, but the fact that the functional orientation was largely still able to correct for this implies that the effect of smaller shifts or misplacements would be effectively minimized with this method.

Calculating angular excursions assuming sensor axes aligned with the typical IMU orientation may be seen as an exaggerated comparison. We calculated excursions in this manner to demonstrate differences as if an experimenter were unaware the sensor moved. This assumption is realistic as it would be difficult to identify changes in placement because sensor movement is rarely about a single axis or of a magnitude approaching 90° about one axis. Additionally, this design allowed us to test the extent to which the functional orientation can correct for extreme sensor misplacement. Another possible limitation is that both groups were healthy with an absence of gait abnormalities. We believe the functional orientation method would work similarly regardless of abnormalities as the orientation is based on subject-specific gait patterns.

Demonstrating the extent to which functional orientation minimizes the effect of varying sensor location is an important step towards collecting reliable free-living gait data. The demonstrated walking- and toe-touch-based functional orientation can correct for shifts in sensor location, as long as sensors avoid areas of large soft tissue deformation. This relatively easy-to-implement functional orientation method is a promising method for application in unobserved, free-living data collection.

References:

[1] L. Pacher, C. Chatellier, R. Vauzelle, L. Fradet, Sensor-to-Segment Calibration Methodologies for Lower-Body Kinematic Analysis with Inertial Sensors: A Systematic Review, Sensors. 20 (2020) 3322. https://doi.org/10.3390/s20113322.

[2] R.V. Vitali, N.C. Perkins, Determining anatomical frames via inertial motion capture: A survey of methods, J. Biomech. 106 (2020) 109832. https://doi.org/10.1016/J.JBIOMECH.2020.109832.

[3] H. Dejnabadi, B.M. Jolles, K. Aminian, A new approach to accurate measurement of uniaxial joint angles based on a combination of accelerometers and gyroscopes, IEEE Trans. Biomed. Eng. 52 (2005) 1478–1484. https://doi.org/10.1109/TBME.2005.851475.

[4] P. Picerno, A. Cereatti, A. Cappozzo, Joint kinematics estimate using wearable inertial and magnetic sensing modules, Gait Posture. 28 (2008) 588–595. https://doi.org/10.1016/j.gaitpost.2008.04.003.

[5] T. Sun, H. Li, Q. Liu, L. Duan, M. Li, C. Wang, Q. Liu, W. Li, W. Shang, Z. Wu, Y. Wang, Inertial Sensor-Based Motion Analysis of Lower Limbs for Rehabilitation Treatments, J. Healthc. Eng. 2017 (2017) 1–11. https://doi.org/10.1155/2017/1949170.

[6] S.M. Cain, R.S. McGinnis, S.P. Davidson, R.V. Vitali, N.C. Perkins, S.G. McLean, Quantifying performance and effects of load carriage during a challenging balancing task using an array of wireless inertial sensors, Gait Posture. 43 (2016) 65–69. https://doi.org/10.1016/j.gaitpost.2015.10.022.

[7] J. Favre, R. Aissaoui, B.M. Jolles, J.A. de Guise, K. Aminian, Functional calibration procedure for 3D knee joint angle description using inertial sensors, J. Biomech. 42 (2009) 2330–2335. https://doi.org/10.1016/j.jbiomech.2009.06.025.

[8] L.S. Vargas-Valencia, A. Elias, E. Rocon, T. Bastos-Filho, A. Frizera, An IMU-to-Body Alignment Method Applied to Human Gait Analysis, Sensors. 16 (2016) 2090. https://doi.org/10.3390/s16122090.

[9] T. McGrath, L. Stirling, Body-Worn IMU Human Skeletal Pose Estimation Using a Factor Graph-Based Optimization Framework, Sensors. 20 (2020) 6887. https://doi.org/10.3390/s20236887.

[10] T. Seel, T. Schauer, J. Raisch, Joint axis and position estimation from inertial measurement data by exploiting kinematic constraints, in: 2012 IEEE Int. Conf. Control Appl., 2012: pp. 45–49. https://doi.org/10.1109/CCA.2012.6402423.

[11] T. Seel, J. Raisch, T. Schauer, IMU-Based Joint Angle Measurement for Gait Analysis, Sensors. 14 (2014) 6891–6909. https://doi.org/10.3390/s140406891.

[12] I. Weygers, M. Kok, T. Seel, D. Shah, O. Taylan, L. Scheys, H. Hallez, K. Claeys, In-vitro validation of inertial-sensor-to-bone alignment, J. Biomech. (2021).

[13] J. Favre, B.M. Jolles, R. Aissaoui, K. Aminian, Ambulatory measurement of 3D knee joint angle, J. Biomech. 41 (2008) 1029–1035. https://doi.org/10.1016/j.jbiomech.2007.12.003.

[14] A.G. Cutti, A. Ferrari, P. Garofalo, M. Raggi, A. Cappello, A. Ferrari, 'Outwalk': a protocol for clinical gait analysis based on inertial and magnetic sensors, Med. Biol. Eng. Comput. 48 (2010) 17–25. https://doi.org/10.1007/s11517-009-0545-x.

[15] J.F. Hafer, S.G. Provenzano, K.L. Kern, C.E. Agresta, J.A. Grant, R.F. Zernicke, Measuring markers of aging and knee osteoarthritis gait using inertial measurement units, J. Biomech. 99 (2020) 109567. https://doi.org/10.1016/J.JBIOMECH.2019.109567.

[16] J. Lebleu, T. Gosseye, C. Detrembleur, P. Mahaudens, O. Cartiaux, M. Penta, Lower Limb Kinematics Using Inertial Sensors during Locomotion: Accuracy and Reproducibility of Joint Angle Calculations with Different Sensor-to-Segment Calibrations, Sensors. 20 (2020) 715. https://doi.org/10.3390/s20030715.

[17] T. McGrath, R. Fineman, L. Stirling, An Auto-Calibrating Knee Flexion-Extension Axis Estimator Using Principal Component Analysis with Inertial Sensors, Sensors. 18 (2018) 1882. https://doi.org/10.3390/s18061882.

[18] M. Nazarahari, H. Rouhani, Semi-Automatic Sensor-to-Body Calibration of Inertial Sensors on Lower Limb Using Gait Recording, IEEE Sens. J. 19 (2019) 12465–12474. https://doi.org/10.1109/JSEN.2019.2939981.